The Asiago-ESO/RASS QSO Survey
II. The Southern Sample[1]

A. Grazian

European Southern Observatory, D-85748 Garching bei München

and

Astronomy Department, University of Padua, I-35122 Italy

A. Omizzolo

and

C. Corbally

Vatican Observatory Research Group, University of Arizona, Tucson AZ 85721 USA

S. Cristiani

European Southern Observatory, ST European Coordinating Facility, D-85748 Garching bei München

and

Osservatorio Astronomico di Trieste Via G.B. Tiepolo 11, 34131 Trieste Italy

M. G. Haehnelt

Institute of Astronomy, Madingley Road, Cambridge CB30HA, England

and

E. Vanzella

European Southern Observatory, D-85748 Garching bei München

and

Astronomy Department, University of Padua, I-35122 Italy

ABSTRACT

This is the second paper of a series describing the Asiago-ESO/RASS QSO survey, a project aimed at the construction of an all-sky statistically well-defined sample of very bright QSOs ($B_J \leq 15$). Such a survey is required to remove the present uncertainties about the properties of the local QSO population and constitutes an homogeneous database for detailed evolutionary studies of AGN. We present here the complete Southern Sample, which comprises 243 bright ($12.60 \leq B_J \leq 15.13$) QSO candidates at high galactic latitudes ($|b_{gal}| \geq 30°$). The area covered by the survey is 5660 sq. deg. Spectroscopy for the 137 still unidentified objects has been obtained. The total number of AGN turns out to be 111, 63 of which are new identifications. The properties of the selection are discussed. The completeness and the success rate for this survey at the final stage are 63% and 46%, respectively.

Subject headings: Catalogs - Surveys - Quasars: general

1. Introduction

QSOs are an important astrophysical and cosmological tool: they represent a major source of information about the origin and evolution of the structures in the Universe. They can be used either directly, as tracers of the density peaks, or as cosmic lighthouses, probing the Universe along the line of sight with their conspicuous flow of photons.

Early stages of galaxy formation are probably connected with QSO activity and central BH accretion. In recent years there has been increasing observational evidence that the evolution of normal galaxies and quasars is closely related and that quasars are short-lived. The evolution of the global star formation rate of the Universe, the space density of starbursting galaxies and that of luminous QSOs appear to be remarkably similar. Recently Kormendy (2000a) proposed that such "monsters" could be set at the heart of galaxy formation. A number of models indeed relate QSOs with galaxies both using theoretical (Haehnelt & Kauffmann 2000; Granato et al. 2001; Monaco et al. 2000; Romano et al. 2001) and observational (Gebhardt et al. 2001; Kormendy 2001) arguments. It is generally accepted now that QSO activity, the growth of SMBHs and the formation of spheroids are all closely linked (Kormendy 2000b).

---

[1]Based on observations collected at the European Southern Observatory, Chile (ESO P66.A-0277 and ESO P67.A-0537), with the Arizona Steward Observatory and with National Telescope Galileo (TNG) during AO3 period.

A well defined large sample of bright QSOs at $z \leq 0.3$ is instrumental in confirming or revising our conceptions about the evolution of QSOs and constitutes a significant challenge for any theoretical model. In particular, it provides key informations on the following issues: *what is the typical mass of Dark Matter Halos hosting AGN ? What is the duty cycle for AGN activity ? What is the typical efficiency of the central engine at the various redshifts ?*

It is paradoxical that in the era of 2dF (Croom et al. 2001; Shanks et al. 2000) and SDSS (Fan et al. 2000), with thousands of faint QSOs discovered up to the highest redshifts ($z = 6.28$), the statistical properties of the QSO population are much better known at $z \sim 2$ than in the local Universe. The aim of this work is to fill this gap with a very large area search for bright and low-z AGN, the Asiago-ESO/RASS QSO Survey (hereafter AERQS). At present, the Northern Sample described in Grazian et al. (2000) (hereafter Paper I) is 85% identified and spectroscopic observations have been planned to complete the survey.

The structure of this paper is the following: in § 2 we report on the Southern Photometry used, the selection criteria are described in § 3; § 4 is dedicated to the New Southern Sample and its statistical properties (selections, completeness, efficiency); finally on § 5 we discuss the properties of the completely identified sample, showing the spectra of newly identified AGN and galaxies. We assume $H_0 = 50\ Km\ s^{-1}\ Mpc^{-1}$, $\Omega_m = 1.0$ and $\Omega_\Lambda = 0.0$. A detailed treatment of the LF and clustering properties of AGN is left to forthcoming papers.

2. The Southern Photometry

The surface density of bright AGN at low redshift is very small, around $10^{-2} sq.\ deg.^{-1}$ as shown in Fig. 1. In practice, to reach significant statistics, an area comparable with the whole sky has to be covered. In Paper I we have discussed a number of databases sampling a wide domain in the electro-magnetic (e.m.) spectrum for the selection of an all-sky sample of optically bright QSOs with a high level of completeness and success rate.

In the northern part of the AERQS the basis of the optical photometry was chosen to be the US Naval Observatory Catalogue (USNO-1A[2]) and the Guide Star Catalogue (GSC-1[3]) with a typical error of 0.2-0.3 in magnitude. For the Southern Sample we have tried to improve the optical photometry, using the positions and optical magnitudes derived from the Digitized Sky Survey (DSS[4]). For each target of interest (the selection is described in § 3) all

[2] *http://archive.eso.org/servers/usnoa-server*

[3] *http://www-gsss.stsci.edu/gsc/gsc12/*

[4] *http://archive.eso.org/dss/dss*

the objects with known B_J magnitudes within a radius of 1.5 arcmin were extracted from the GSC Catalogue. Small scans of the target and the GSC calibrating objects were extracted from the DSS plates. Instrumental magnitudes were then computed by aperture photometry in a circular area of 7.5 arcsec radius (9 DSS pixels diameter). A polynomial calibration curve is used to interpolate the magnitudes of the target. A typical calibration curve is shown in Fig. 2. We have tested the accuracy of this procedure using 446 photometric standards of the input catalogue used to calibrate the photometric material of the Homogeneous Bright QSO Survey (Cristiani et al. 1995), deriving a σ_{B_J} of 0.10 *mag* in the interval $12.0 \leq B_J \leq 15.5$.

The 7.5 arcsec aperture size (corresponding to a radius of 18.5 Kpc at $z = 0.1$) is the result of a trade-off between the attempt to estimate nuclear magnitudes for our AGN (reducing the contribution of the host galaxy) and the necessity of a photometry that is "robust" against errors in the centering of the aperture. By comparing our photometry with the GSC2 catalogue we find, for the 80 AGN of Tab. 1 that have GSC2 J magnitudes, a mean difference $< J_{GSC2} - B_J >= 0.10$ with a scatter of 0.4 mag, which can be ascribed to photometric errors and AGN variability. Using larger apertures obviously increases the contribution of the host galaxy. For example if we compare the magnitudes obtained with a 7.5 arcsec circular aperture with the magnitudes in a 15 arcsec aperture, for the 111 AGN of Tab. 1 we obtain a $< B_J(7.5) - B_J(15.0) >= 0.5$ with a scatter of 0.4.

We have used only plates based on *IIIaJ* emulsion to compute the magnitudes, as other emulsions are not standard and difficult to calibrate. This, together with the selection criteria described below, is the source of non uniformity of the sky coverage. Fig. 3 shows the area of the sky covered by the present survey. Table 2 provides a list of the sky sub-areas plotted in Fig. 3, which total 5660 sq. deg. of the Southern Hemisphere.

3. The Selection Criteria

QSO candidates have been selected by cross correlating the X-ray sources in the ROSAT All Sky Survey Bright Source Catalog (RASS-BSC, Voges et al. (1999)) with optically bright objects in the DSS plates. As stated in Paper I, given the low surface density of local bright AGN, misidentifications are very unlikely since we adopt a matching radius that is three times the RMS positional uncertainty of each X-ray source (typically 15-20 *arcsec*).

We want to stress here that this survey aims at finding *optically bright* QSOs and the X-ray emission is used only to compute an "X-Optical color" for the selection of AGN. Therefore the result of our selection cannot be considered an identification of X-ray sources. This makes the follow-up spectroscopy quicker than in the case of optical identifications of

X-ray sources, because we do not care about objects fainter than the chosen optical flux limits and mis-identifications of optically fainter X-ray sources have no effect on the result.

We applied to the X-ray catalogue a number of criteria that do not affect drastically the completeness of our survey (basically the same used in Paper I): exposure time $t_{exp} \geq 300s$, Galactic latitude $|b_{gal}| \geq 30°$, hardness ratio in the 0.5÷2.0 and 0.1÷0.4 keV energy bands $-0.9 \leq HR1 \leq +0.9$, hardness ratio in the 0.9÷2.0 and 0.5÷0.9 keV energy bands $-0.6 \leq HR2 \leq +0.8$, likelihood of extent $lik_{ext} \leq 35$ to avoid extended X-ray sources; this corresponds to a limit for source extent $ext \leq 100$ in agreement with the preliminary results of the North Ecliptic Pole (NEP) survey (Voges et al. (2001) and C. Mullis private communications, 2001). In addition the likelihood of detection $lik_{det} \geq 25$ to select only reliable sources, with a significant level of detection in the RASS-BSC. These parameters have been described extensively in Voges et al. (1999).

Then we apply two basic criteria:

- $12.60 \leq B_J \leq 15.13$

and

- $a_{ox} \leq 1.9$

where $a_{ox} = -0.438 log_{10}(cps) - 0.193 B_J + 4.20$ and cps is the X-ray flux measured in counts per second.

We have used the selection criterion $\alpha_{ox} \leq \alpha_{max}$ which, as shown in Fig. 1 of Paper I, for objects brighter than the adopted optical limits provides a sample with a degree of incompleteness that is not a function of the apparent magnitude. We have compared the present selection with the low redshift ($z \leq 0.3$) optically or IR selected QSOs of the Véron Catalogue (Véron-Cetty & Véron (2001), hereafter VV01): out of the 67 QSOs known within our spatial and optical flux limits, 42 (63 %) meet our selection criteria. Radio or X-ray selected AGN are not taken into account, to avoid biases in the estimation of the completeness.

The adopted selections in lik_{det}, lik_{ext}, $HR1$ and $HR2$ remove 25% of the RASS sources that are probably stars, extended X-ray sources and other spurious contaminants; spectroscopic identifications for these sources are not available. The application of the same criteria for the AGN in the VV01 Catalogue lowers the completeness from 64% to 63%; we can conclude, as in Paper I, that the adopted criteria increase the effectiveness without affecting the completeness.

We have selected a total of 243 candidates in the Southern Hemisphere over ∼5660 *sq. deg.* at high Galactic latitude $|b_{gal}| \geq 30°$. They are listed in Tab. 1.

4. The Southern Sample

Of the 243 candidates belonging to the southern part of the AERQS, 45% had previous spectroscopic identifications in the literature (Véron Catalogue, NED[5]). For the remaining 137 objects we started an observational campaign. We had several runs with different telescopes for a total of 7 nights: Tab. 3 summarizes the observations.

The reduction process used the standard MIDAS facilities (Banse et al. 1983) and other useful software available at ESO Garching through the SCISOFT[6] environment. The raw data were sky-subtracted and corrected for pixel-to-pixel sensitivity variations by division with a suitably normalized exposure of the spectrum of an incandescent source (flat-field). The wavelength calibration was carried out by comparison with exposures of He and Ne lamps. Relative flux calibration was carried out by observations of spectrophotometric standard stars (Oke 1990). For extended objects, only the core/nucleus flux was considered.

The identification classes reported in Table 1 are: AGN = Active Galactic Nucleus; $STAR$ = star; GAL = galaxy; $BLLAC$ = BL Lac object.

Objects with emission lines were classified as AGN only if they show broad and/or strong lines (typically H_α, H_β or Mg II). Galaxies with a weak ($EW \leq 12\mathring{A}$) unresolved H_α and no other features of AGN activity are classified as $EM\ GAL$ and, together with the newly identified AGN or normal galaxies, are shown in Fig.4,5,6,7,8,9. The objects classified as BL Lacs in Tab. 1 were already known from the literature (VV01 Catalogue). In the next section we will describe more in detail the emission line galaxies and try to interpret their properties.

At the end of our spectroscopic campaign we have carried out 137 new identifications; we have discovered more than 60 new AGN, significantly enlarging the number of bright QSOs at $z \leq 0.3$. Fig. 10 shows the redshift distribution of the AGN in this sample.

---

[5] *http://nedwww.ipac.caltech.edu/*

[6] *http://www.eso.org/science/scisoft/*

5. Discussion

We have found 111 AGN out of 243 candidates, corresponding to a success rate of 46%. Stars are the mean source of contamination, especially active M stars, which are powerful X-ray emitters compared to their optical magnitudes, resembling the a_{ox} of AGN. To distinguish them effectively an optical color, for example $B-R$, would be extremely useful as these two classes have typically different optical spectral energy distributions. We have obtained J and F magnitudes, equivalent to B and R respectively, from the GSC-2[7] catalogue for all the object of this survey. In Fig. 11 the $J-F$ color distribution is plotted for different classes of objects. We have divided AGN into two classes "Point-like" and "Extended" or "Galaxy-like" according to the classification given in the GSC-2 catalogue. There is no evident difference in colors between these two classes. AGN and normal stars are not so different in $J-F$. M-stars, instead, can be easily separated from AGN. With the application of a reasonable cut in the optical color ($J-F \leq 1.6$) the success rate of the present survey would be increased from the present value of 46% to 63% but the completeness would be affected as well, decreasing from 63% to a value of 40%. If we compare the "Extended" and "Point-like" AGN of Fig. 11, a Kolmogorov-Smirnov test gives a probability of 89% that the two samples are extracted from the same population. The mean values of $J-F$ for the two samples are similar (0.69 and 0.72 for "Extended" and "Point-like", respectively) and the dispersion is slightly larger for the "Extended" objects.

A more important consideration is the fact that surveys based only on optical colors, assuming typical blue SEDs for AGN, are significantly incomplete especially at low redshift and at faint absolute magnitudes, where the host galaxy contribution starts to be relevant. Fig. 12 shows the dependence of the AGN color $J-F$ on absolute magnitude M_B: faint Nuclei tend to be redder than the bright QSOs. In Fig. 13 we show the $J-F$ color distribution for 30 QSOs with $z \leq 0.3$ in the PG Survey (Schmidt & Green 1983). We compare it with the same distribution for 80 AGN in the AERQS Survey with $z \leq 0.3$: an extended tail towards the red $J-F$ color for the X-ray selected AGN is evident. PG QSOs have typically a blue optical color ($J-F \leq 1.04$). If we had selected only AGN bluer than $J-F \leq 1.04$, 22 (28%) objects would have been missed.

Two effects can determine the big spread in the observed $J-F$ color: the starlight contamination of the host galaxy and the existence of intrinsically red Active Galactic Nuclei. An additional contribution can be due to QSO variability, whose effect is difficult to address in detail, as it significantly depends on the time lag between the different flux measurements. From the analysis of the structure function (Cristiani et al. 1996) we should expect an average

---

[7] *http://www-gsss.stsci.edu/gsc/gsc2/GSC2home.htm*

uncertainty on the $J-F$ color due to variability of 0.2 mag for QSOs with a typical absolute magnitude $M_B \sim -25$ and 0.3 for $M_B \sim -23$.

The contribution of the host galaxy is clearly visible in Fig. 14, where we have normalized and stacked all QSO spectra obtained in this survey. We compare the result with the composite spectra by SDSS (Vanden Berk et al. 2001), First Bright Quasar Survey (Brotherton et al. 2001) and with a synthetic spectrum used for photometric redshift studies with a continuum slope of $\nu^{-1.75}$, redder than a typical $\nu^{-1.2}$ Blue QSOs. It is clearly visible in our composite spectrum the red continuum and the strong feature typical of early type galaxies (Ca doublet at 3929.3 and 3963.8 Å), producing a significant absorption in the rest-frame B band. Besides, it is apparent that for QSOs fainter than $M_B = -24$ the contribution of the host galaxy produces a redder SED with respect to QSOs brighter than $M_B = -24$. K-corrections are computed following the recipe of Cristiani & Vio (1990), but based on the new QSO composite spectra (FBQS and SYNT) plotted in Fig. 14.

In Fig. 15 we have tried to model the pattern of $J-F$ color observed in Fig. 12. To reproduce the full range in $J-F$ color, both a contamination from the host galaxy and the existence of AGN bluer and redder than the adopted composite spectra are necessary. QSO variability and photometric errors are expected to increase the scatter observed in Fig. 12 with respect to Fig. 15. Clearly the synthetic QSO spectrum is too red with respect to the observed $J-F$ distribution, while the FBQS composite spectrum is roughly in agreement with the observations (a slightly bluer QSO spectrum would produce an even better match). A morphological analysis of individual cases is required in order to quantify the relative incidence of these effects.

There are 5 objects with H_α in emission, faint [O III] doublet and no other signature of AGN activity. We have classified them as *EM GAL* in Table 1. They could be special cases, for example AGN obscured by dusty torus, according to the unified model. Another possibility is that they are normal starbursts or liners, common in a soft X-ray survey like the ROSAT sample. Further analysis, for example using hard X-ray observations with Chandra or XMM-Newton, can shed light on their nature and disentangle between Starburst and AGN activity. In the following papers only objects classified as bona-fide *AGN* will be taken into account to study properties like clustering or Luminosity Function.

The LogN-LogS relation for AGN belonging to this sample is shown in Fig. 1 and compared with the relation found by Köhler et al. (1997) for QSOs with $0.07 \leq z \leq 2.2$. It is also consistent with the same relation found for the northern part of the AERQS.

With the completion of the southern part of the AERQS a statistically well-defined set of 340 bright QSOs with $z \leq 0.3$ has been collected. **On the basis of the measured**

success rate, at the end of the present project, we expect to provide a full-sky "local" sample of 400 AGN.

We warmly thank the referee for carefully reading the manuscript, for useful suggestions and for improving significantly the quality of this paper. Part of the work has been supported by the European Community Research and Training Network "Physics of the Intergalactic Medium". AG was supported by the ESO DGDF 2000 and by an ESO Studentship and acknowledges the generous hospitality of ESO headquarters during his stay at Garching. It is a pleasure to thank R. Mignani for his invaluable help with the GSC-2 and A. Goncalves Darbon for her precious suggestions on objects classifications and interesting discussions. This project has been supported by the European Commission through the "Access to Research Infrastructures Action of the Improving Human Potential Programme", awarded to the 'Instituto de Astrofísica de Canarias' to fund European Astronomers access to the European Northern Observatory, in the Canary Islands. This paper makes use of the ROSAT All-Sky Survey Bright Source Catalogue (1RXS). The Guide Star Catalogue-II (GSC-2) is a joint project of the Space Telescope Science Institute and the Osservatorio Astronomico di Torino. Space Telescope Science Institute is operated by the Association of Universities for Research in Astronomy, for the National Aeronautics and Space Administration under contract NAS5-26555. The participation of the Osservatorio Astronomico di Torino is supported by the Italian Council for Research in Astronomy. Additional support is provided by European Southern Observatory, Space Telescope European Coordinating Facility, the International GEMINI project and the European Space Agency Astrophysics Division. Based on photographic data obtained using the UK Schmidt Telescope. The UK Schmidt Telescope was operated by the Royal Observatory Edinburgh, with funding from the UK Science and Engineering Research Council, until 1988 June, and thereafter by the Anglo-Australian Observatory. Original plate material is copyright the Royal Observatory Edinburgh and the Anglo-Australian Observatory. The plates were processed into the present compressed digital form with their permission. The Digitized Sky Survey was produced at the Space Telescope Science Institute under US Government grant NAG W-2166. This research has made use of the NASA/IPAC Extragalactic Database (NED) which is operated by the Jet Propulsion Laboratory, California Institute of Technology, under contract with the National Aeronautics and Space Administration.

REFERENCES

Banse K., Crane P., Ounnas C. & Ponz D., 1983 Proc. of DECUS, Zurich, p. 87

Brotherton, M. S., Arav, N., Becker, R. H., Tran, H. D., Gregg, M. D., White, R. L., Laurent-Muehleisen, S. A. & Hack, W. 2001 ApJ 546, 775

Cristiani, S. & Vio, R. 1990 å 227, 385

Cristiani, S., La Franca, F., Andreani, P., Gemmo, A., Goldschmidt, P., Miller, L., Vio, R., Barbieri, C., Bodini, L., Iovino, A., Lazzarin, M., Clowes, R.G., MacGillvray, H., Gouiffes, C., Lissandrini, C. & Savage, A. 1995 A&A 112, 347

Cristiani, S., Trentini, S., La Franca, F., Aretxaga, I., Andreani, P., Vio, R. & Gemmo, A. 1996 A&A 306, 395

Cristiani, S., Grazian, A., Omizzolo, A. & Corbally, C., astro-ph/0010562; Proceedings of the MPA/ESO/MPE Joint Astronomy Conference "Mining The Sky", July 31 - August 4, 2000, Garching, Germany

Croom, S. M., Smith, R. J., Boyle, B. J., Shanks, T., Loaring, N. S., Miller, L. & Lewis, I. J. 2001 MNRAS 322, 29

Fan et al., 2000 AJ 119, 1

Gebhardt, K., Kormendy, J., Ho, L. C., Bender, R., Bower, G., Dressler, A., Faber, S. M., Filippenko, A. V., Green, R., Grillmair, C., Lauer, T. R., Magorrian, J., Pinkney, J., Richstone, D. & Tremaine, S. 2000 ApJ 543, 5

Granato, G. L., Silva, L., Monaco, P., Panuzzo, P., Salucci, P., De Zotti, G. & Danese, L. 2001 MNRAS 324, 757

Grazian, A., Cristiani, S., D'Odorico, V., Omizzolo, A. & Pizzella, A. 2000 AJ 119, 2540; Paper I

Haehnelt, M. G. & Kauffmann, G. 2000 MNRAS 318, 35

Köhler, T., Groote, D., Reimers, D. & Wisotzki, L. 1997 A&A 325, 502

Kormendy, J., 2000 astro-ph/0007400

Kormendy, J., 2000 astro-ph/0007401; The Seventh Texas-Mexico Conference on Astrophysics: Flows, Blows and Glows (Eds. W. H. Lee and S. Torres-Peimbert) Revista Mexicana de Astronomia y Astrofisica (Serie de Conferencias) Vol. 10, pp. 69-78

Kormendy, J., astro-ph/0105230; In Galaxy Disks and Disk Galaxies, Conference held in Rome, Italy, June 12-16, 2000 at the Pontifical Gregorian University and sponsored by the Vatican Observatory. ASP Conference Series, Vol. 230. Edited by J. G. Funes, S. J. and E. M. Corsini. San Francisco: Astronomical Society of the Pacific 2001, pp. 247-256

Monaco, P., Salucci, P. & Danese, P., 2000 astro-ph/9909267; proceedings of the IGRAP meeting “Clustering at high redshift”, Marseille, June 1999

Oke, J. B., 1990 AJ 99, 1621

Romano, D., Matteucci, F. & Danese, L., astro-ph/0107068; Proceedings of the Workshop “Chemical Enrichment of the ICM and IGM”, Vulcano, May 2001

Shanks, T., Boyle, B.J., Croom, S.M., Loaring, N., Miller, L. & Smith, R.J. 2000 astro-ph/0003206; Mining the Sky, Proceedings of the MPA/ESO/MPE Workshop held at Garching, Germany, 31 July-4 August, 2000. Edited by Springer-Verlag, 2001, p.143

Schmidt, M. & Green, R. F., 1983 ApJ 269, 352

Vanden Berk et al. 2001 AJ 122, 549

Véron-Cetty, M. P. & Véron, P., 2001, Quasars and Active Galactic Nuclei (10th Ed.); ESO Scientific Report 20

Voges, W., Aschenbach, B., Boller, Th., Bräuninger, H., Briel, U., Burkert, W., Dennerl, K., Englhauser, J., Gruber, R., Haberl, F., Hartner, G., Hasinger, G., Krster, M., Pfeffermann, E., Pietsch, W., Predehl, P., Rosso, C., Schmitt, J. H. M. M., Trmper, J. & Zimmermann, H. U., 1999 A&A 349, 389

Voges, W., Henry, J. P., Briel, U. G.; Böhringer, H., Mullis, C. R., Gioia, I. M. & Huchra, J. P., 2001 AJ 553, 119

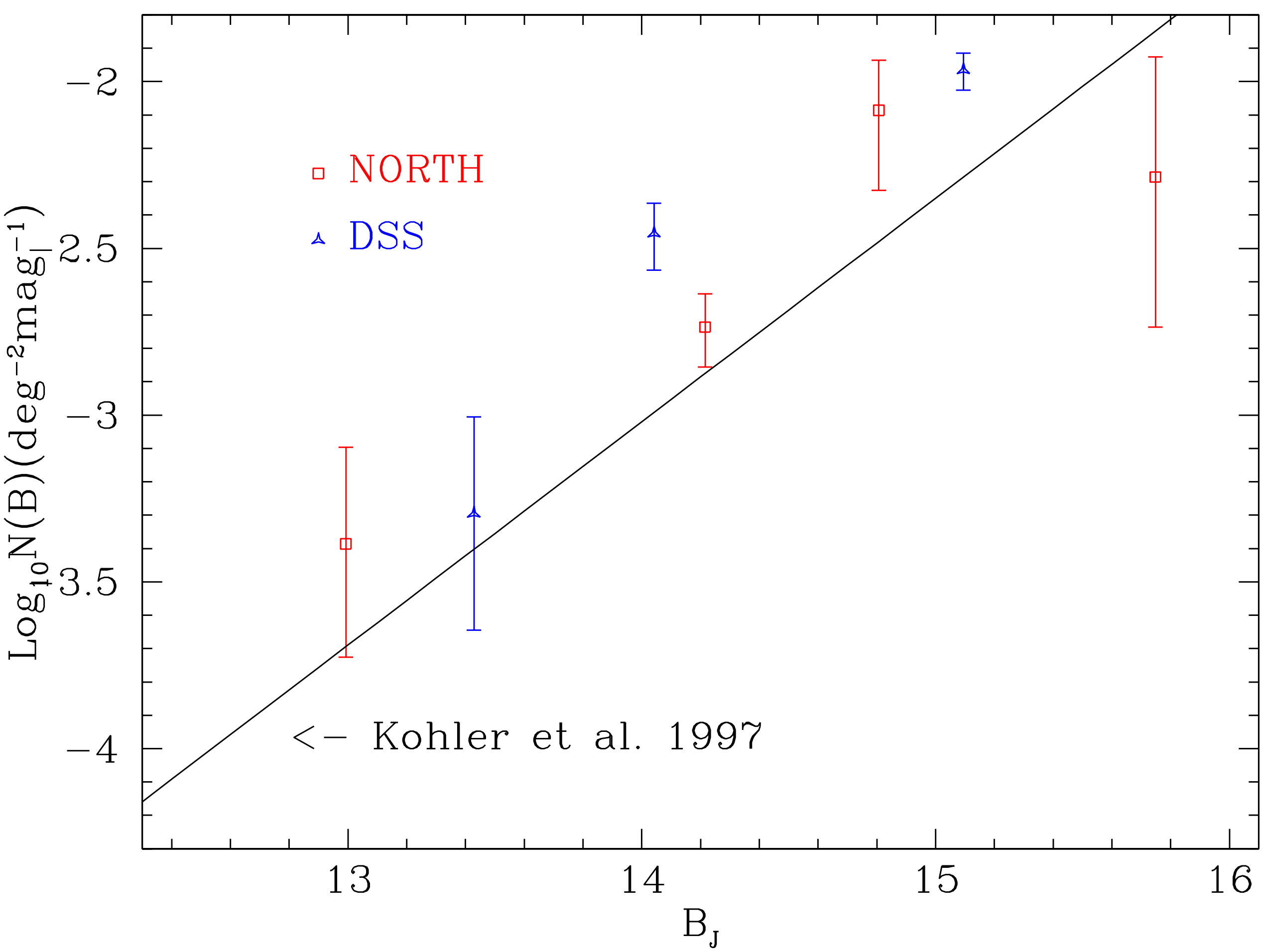

Fig. 1.— The LogN-LogS relation of QSOs. Triangles represent the current sample and are AGN with $0.04 \leq z \leq 0.2$. The open squares are the analogs for the northern part of the AERQS (Grazian et al. 2000). The solid line is the relation found by Köhler et al. (1997) for QSOs with $0.7 \leq z \leq 2.2$.

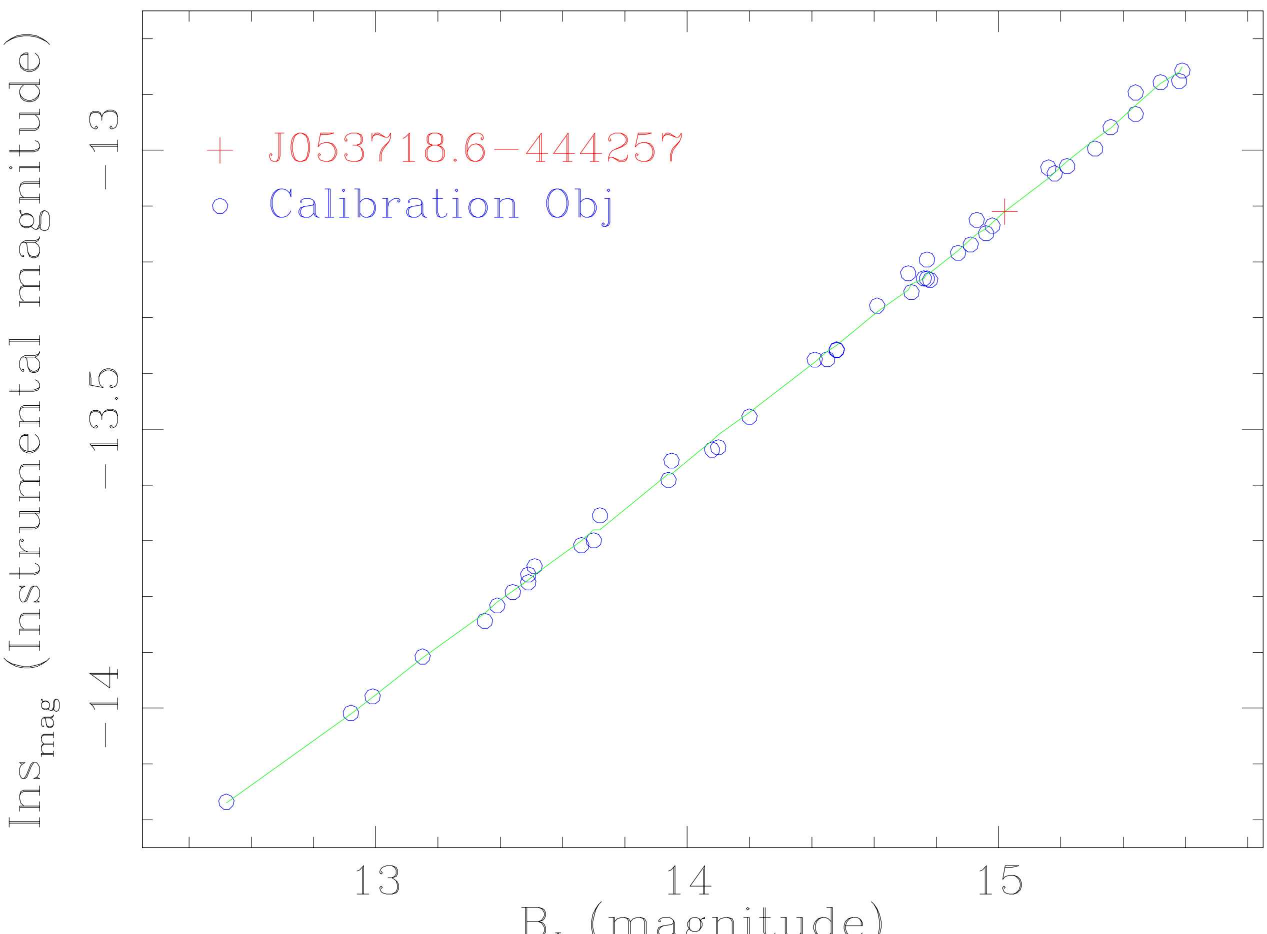

Fig. 2.— A typical calibration curve for one of the AERQS candidates (1RXS-J053718.6-444257). 45 objects with known B_J magnitude from the GSC Catalogue within a radius of 1.5 arcmin. were used to derive the calibration curve.

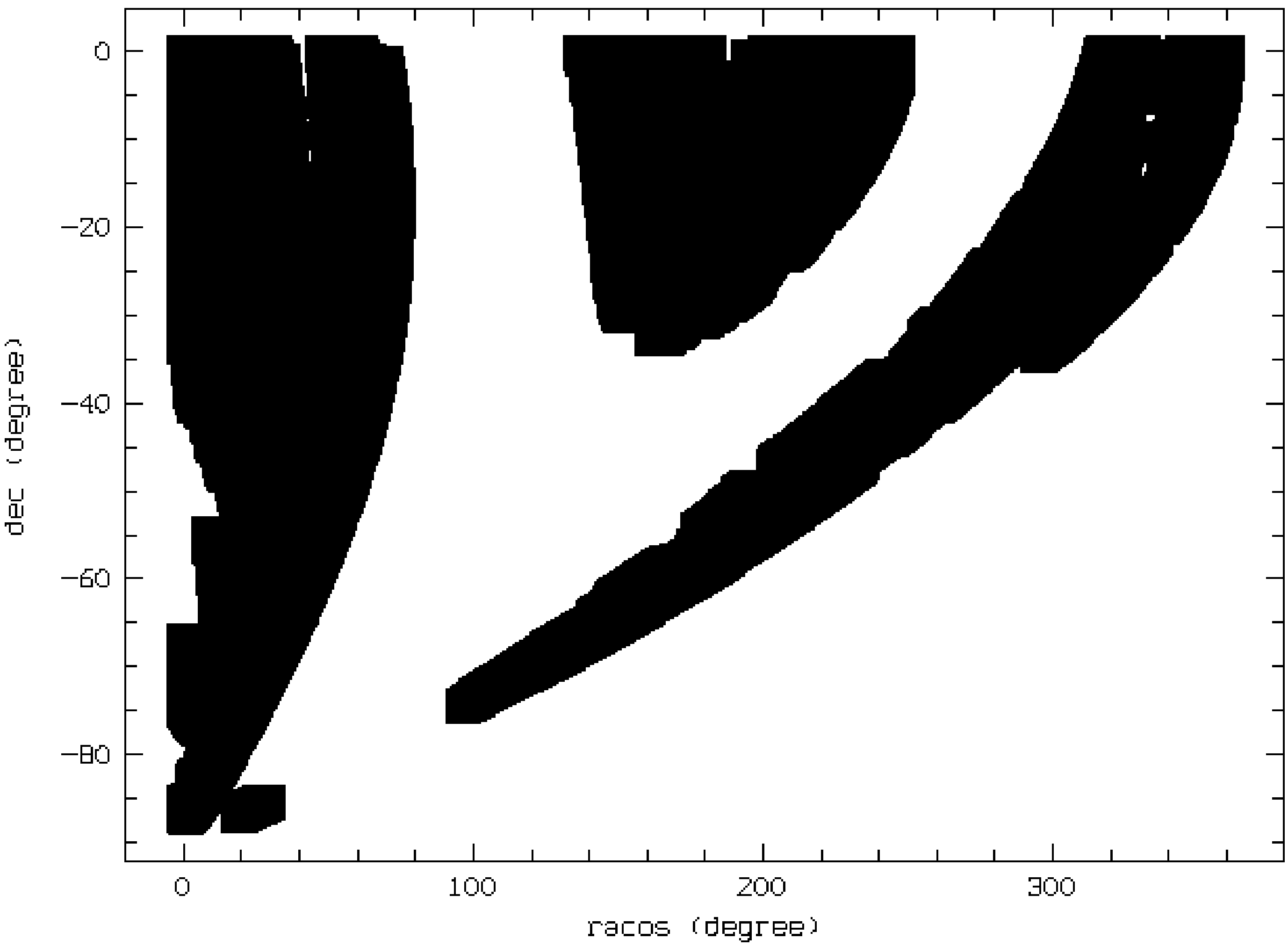

Fig. 3.— The black area shows the regions covered by the present sample after taking into account the selection criteria described in section 2 and 3. The projection of the southern sky is done here in $RA\cos(DEC)$ vs DEC.

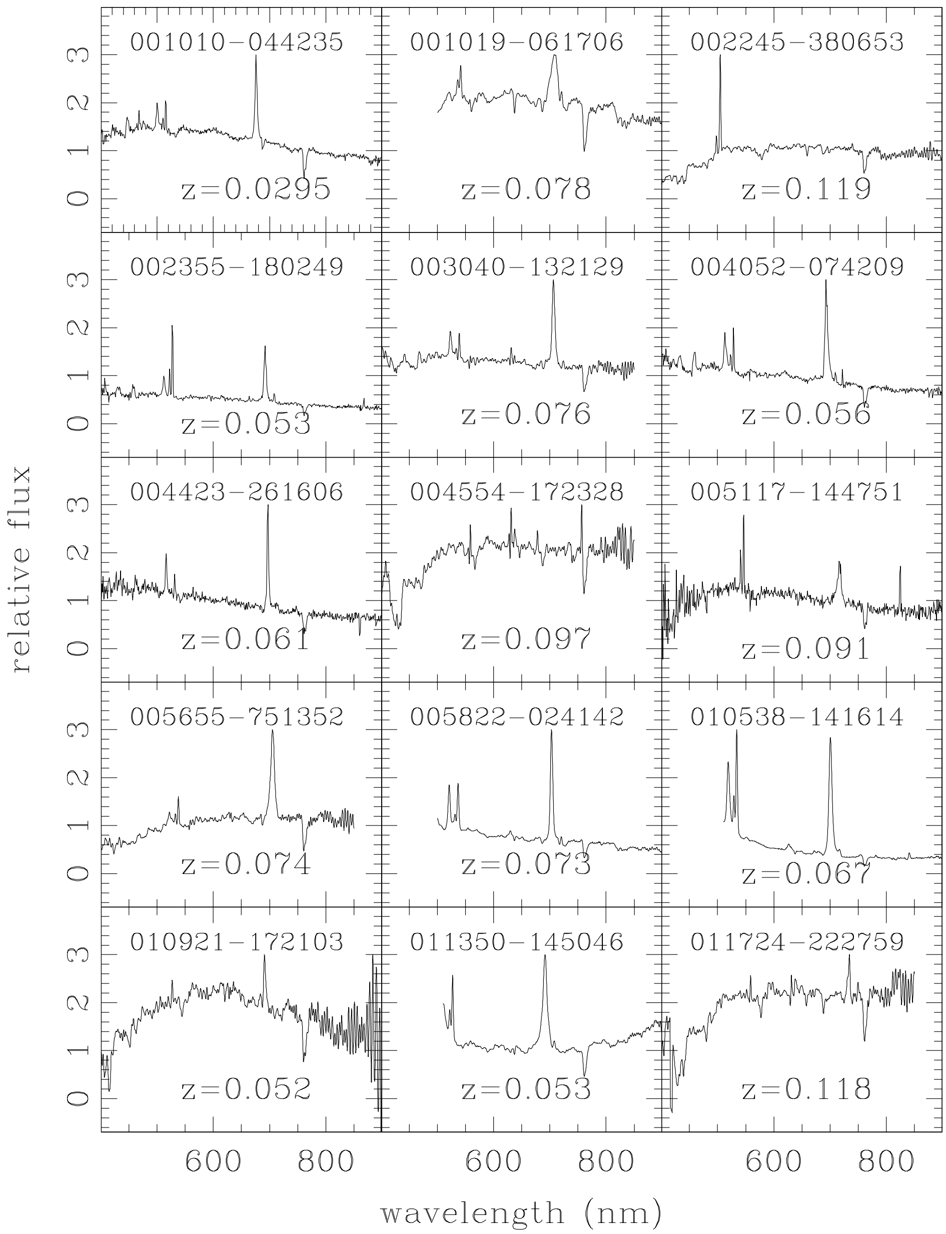

Fig. 4.— Spectra of the newly identified AGN and Galaxies during the present survey.

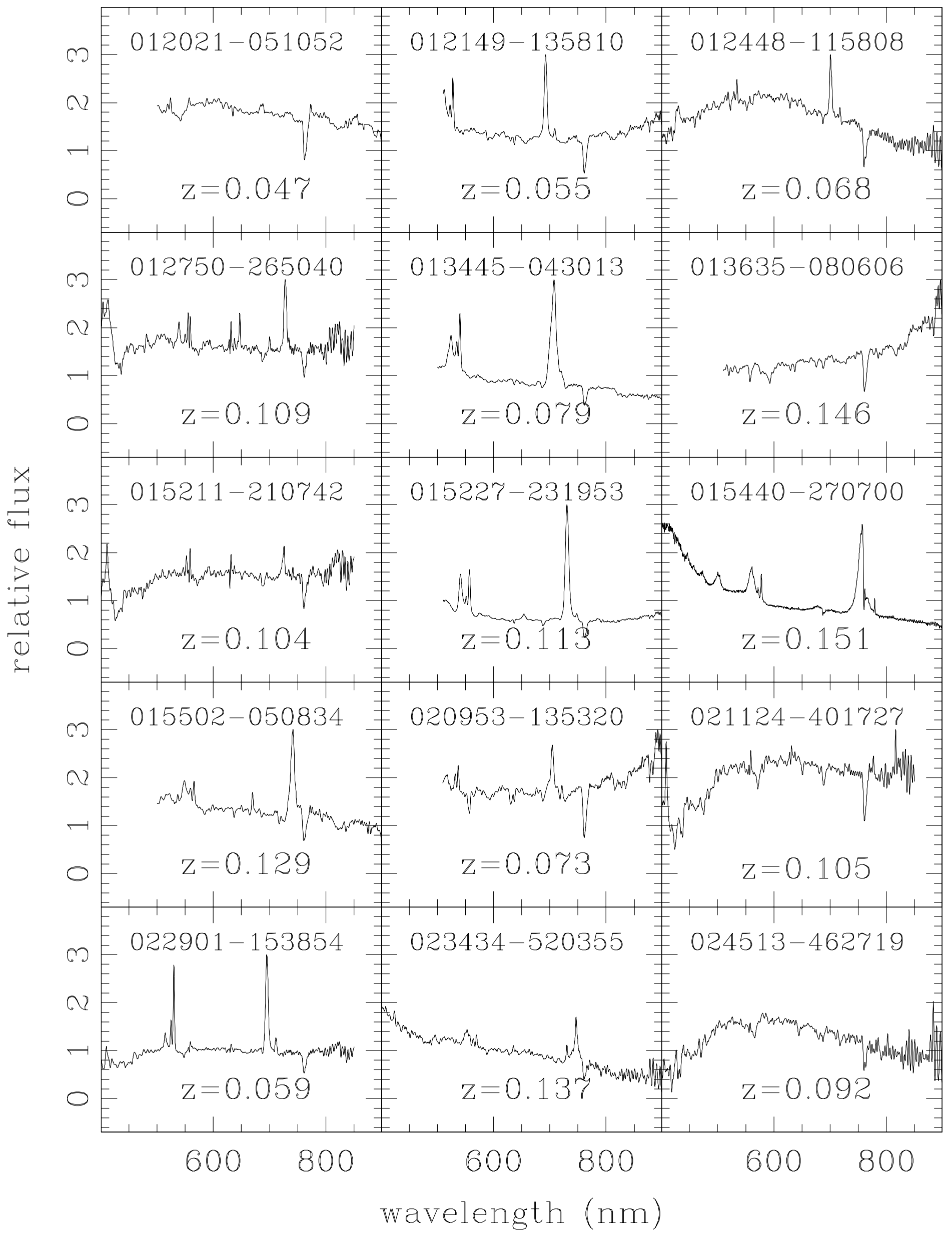

Fig. 5.— Continued.

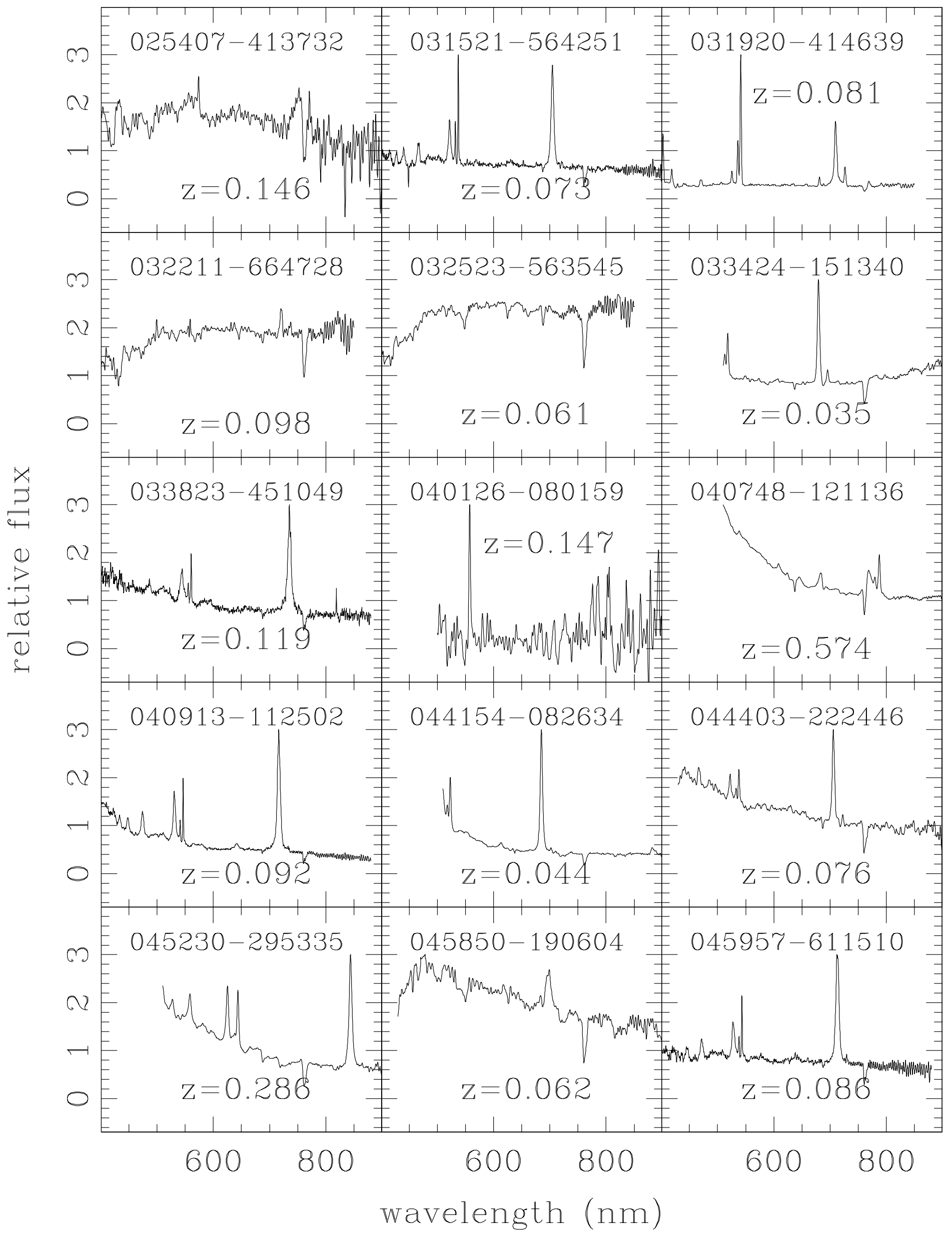

Fig. 6.— Continued.

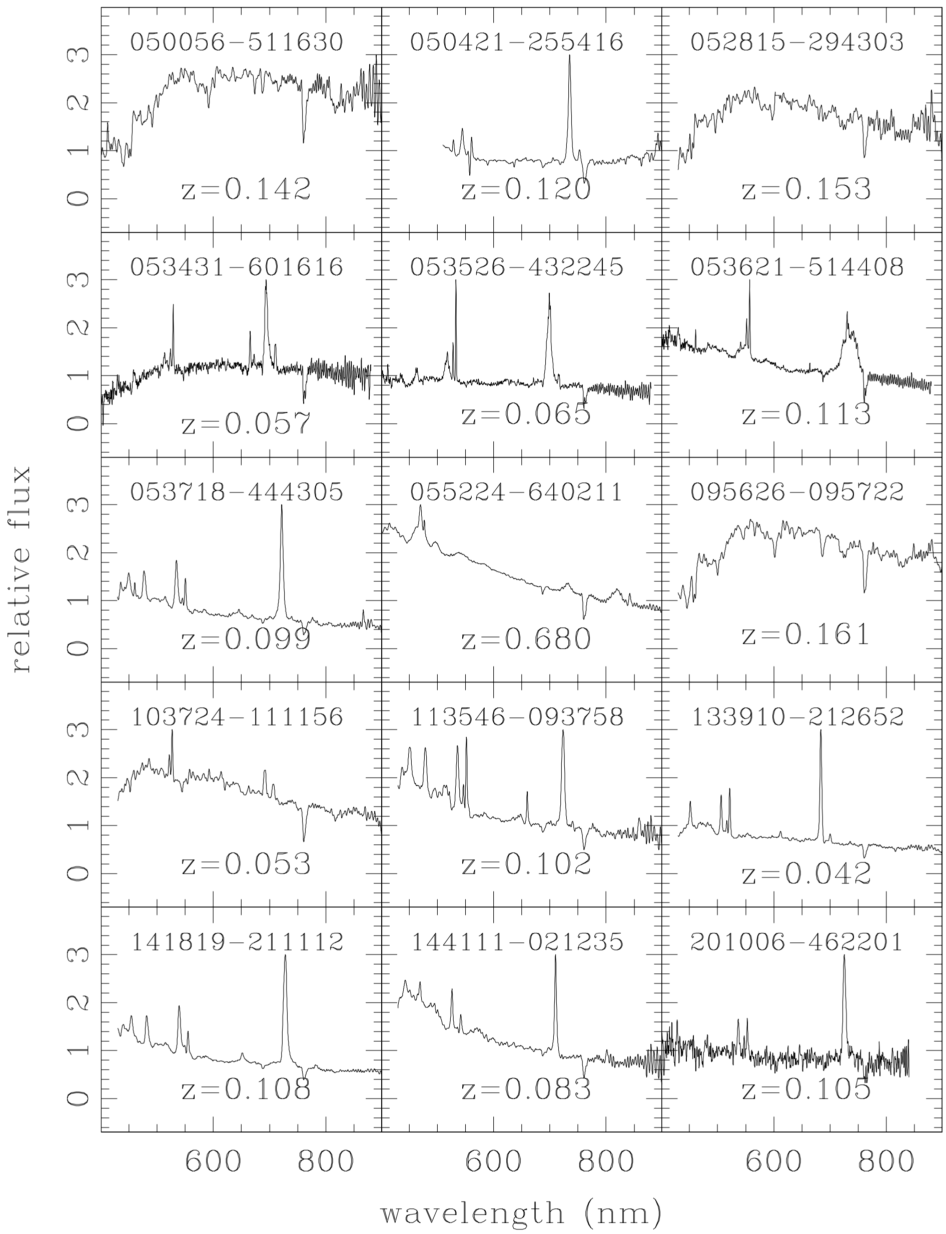

Fig. 7.— Continued.

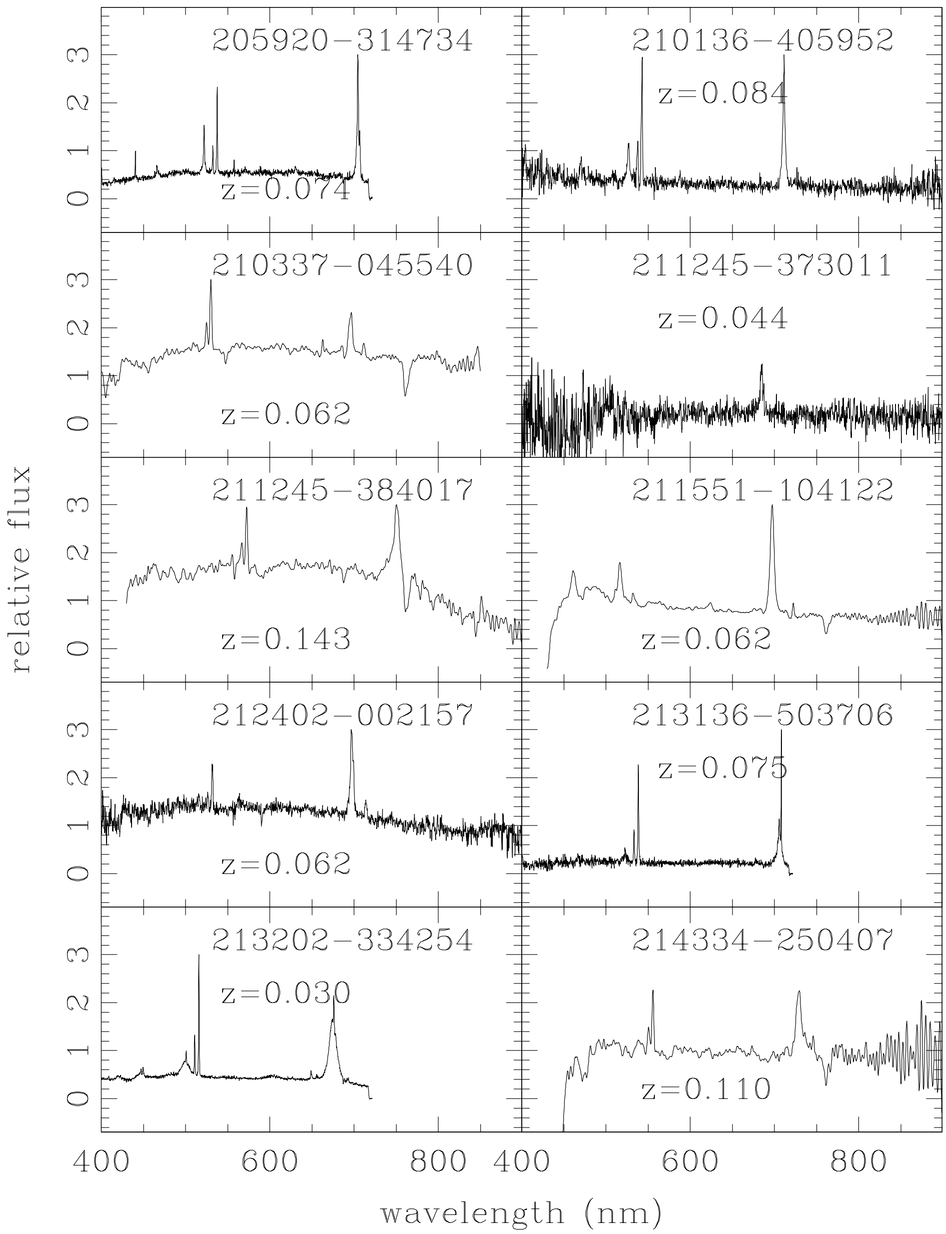

Fig. 8.— Continued.

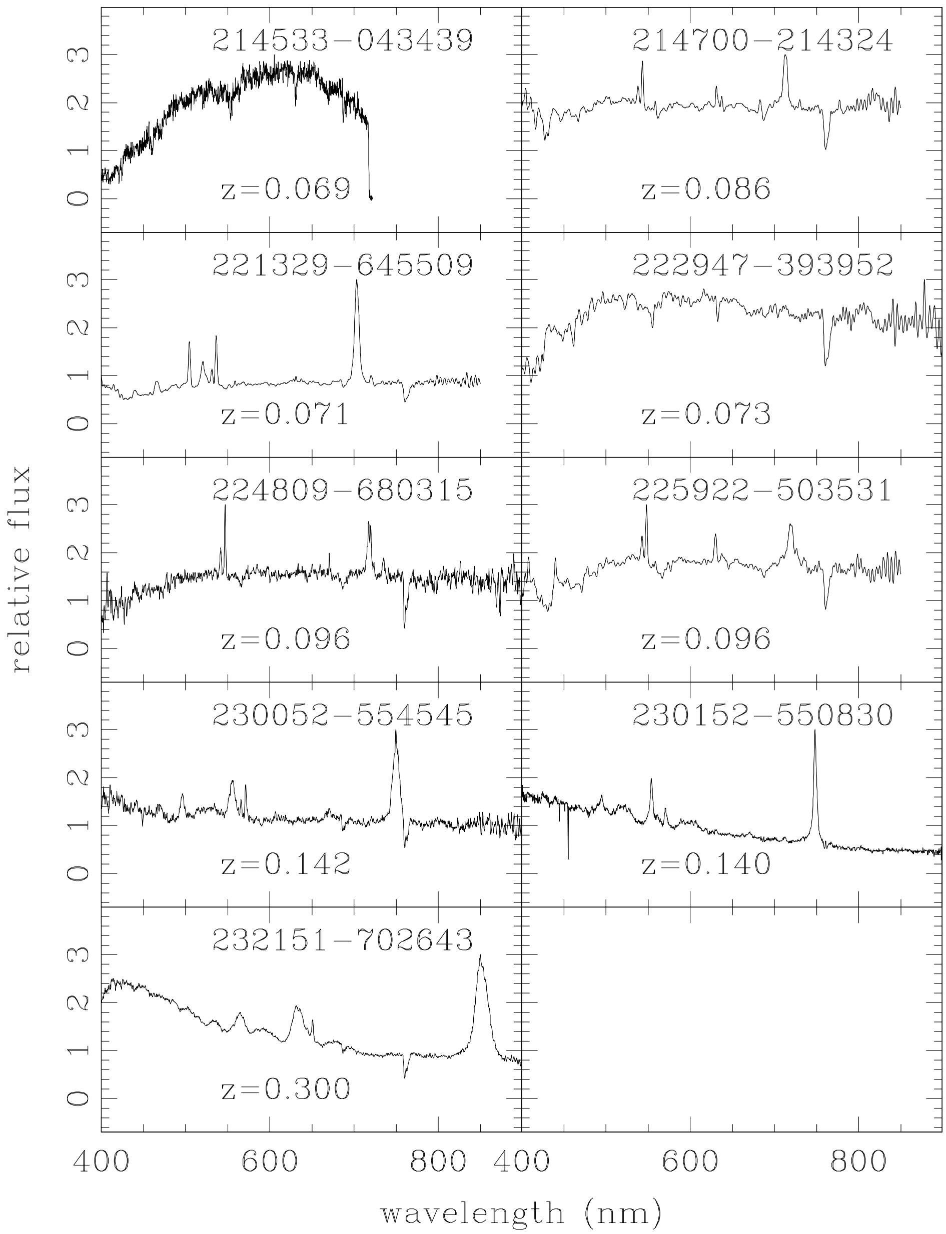

Fig. 9.— Continued.

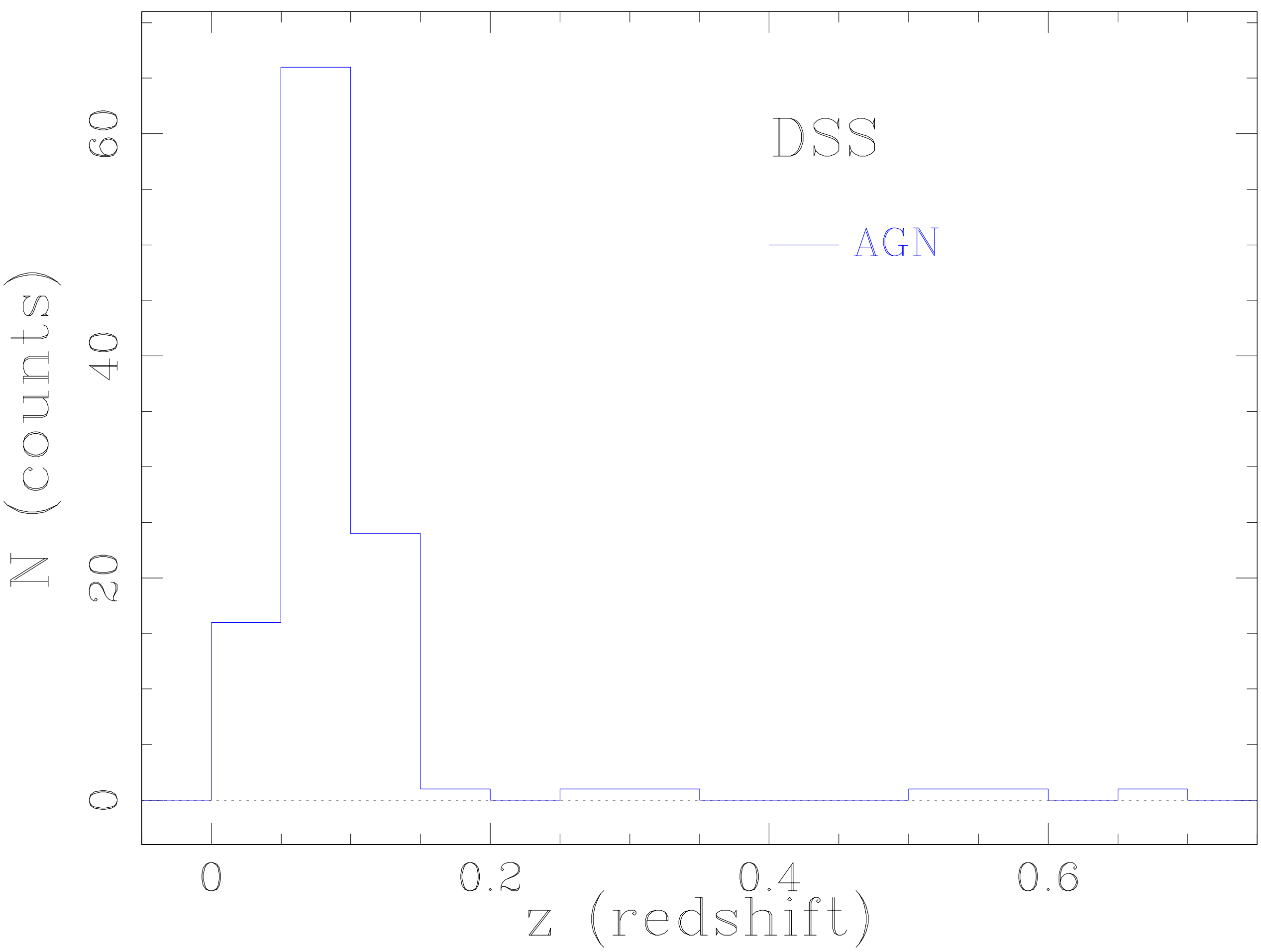

Fig. 10.— The redshift distribution for the AGN in our Southern Sample.

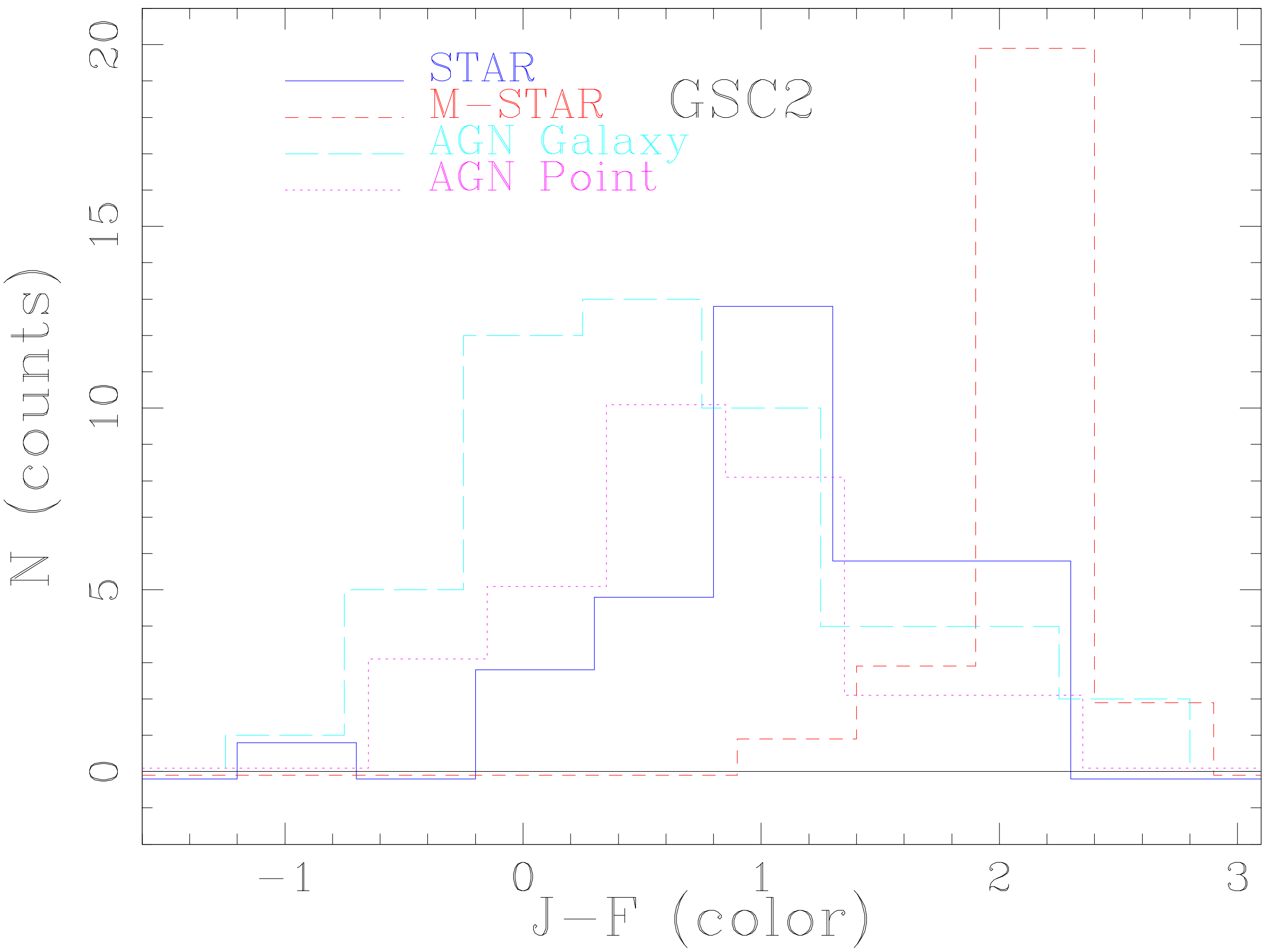

Fig. 11.— The $J - F$ color distribution for AGN, M-stars and normal stars in our Southern Sample. Only M-stars can be separated from AGN with optical color criteria. "AGN Point" refers to AGN classified as point like sources in the GSC-2 catalogue. "AGN Galaxy" are AGN classified as extended sources. Histograms are shifted slightly in x and y directions for clarity.

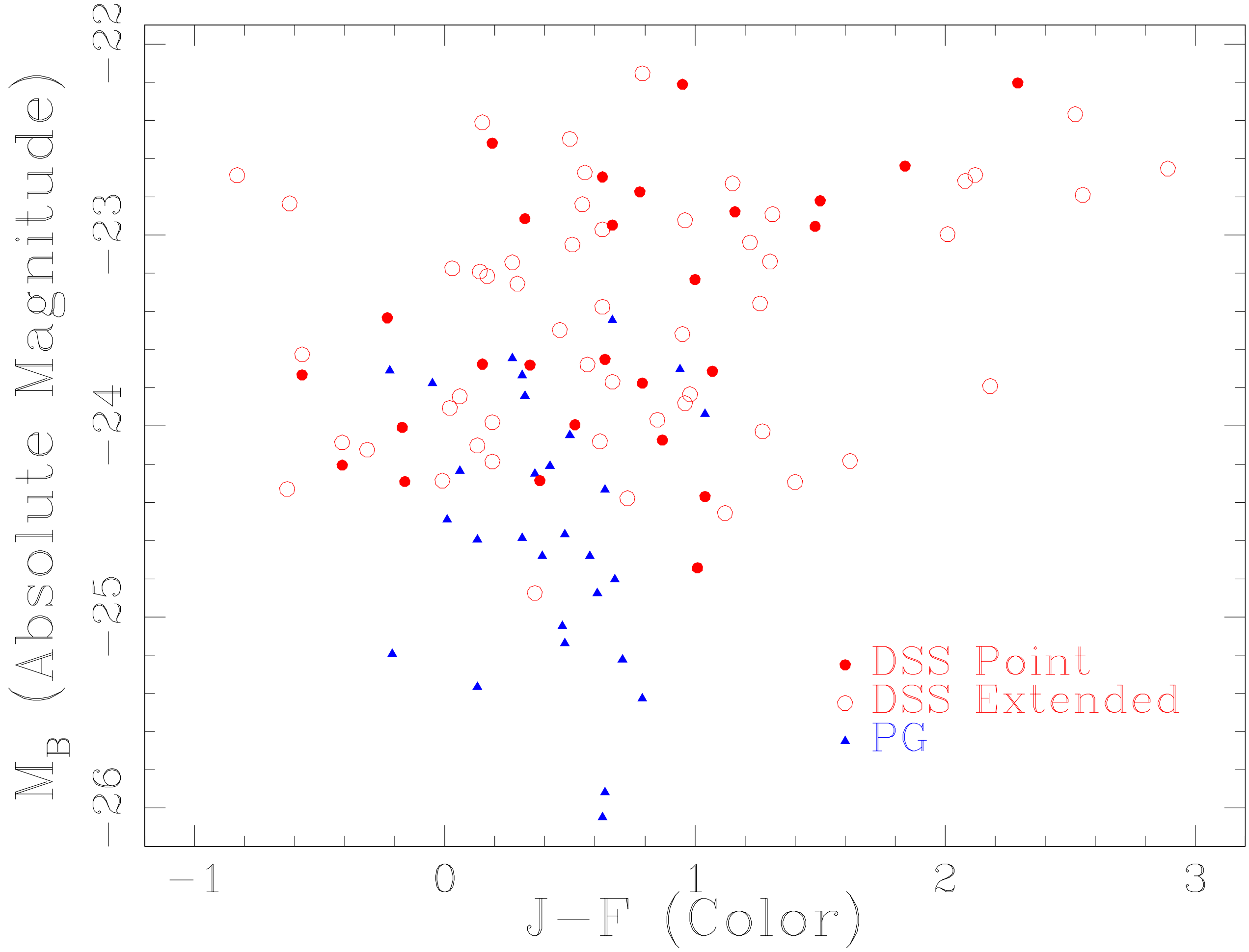

Fig. 12.— The $J - F$ color vs. Absolute Magnitude M_B for AGN in our Southern Sample and for QSOs belonging to the PG survey (Schmidt & Green 1983). Faint Nuclei are redder than bright QSOs: the host galaxy starts to affect the optical color of the AGN.

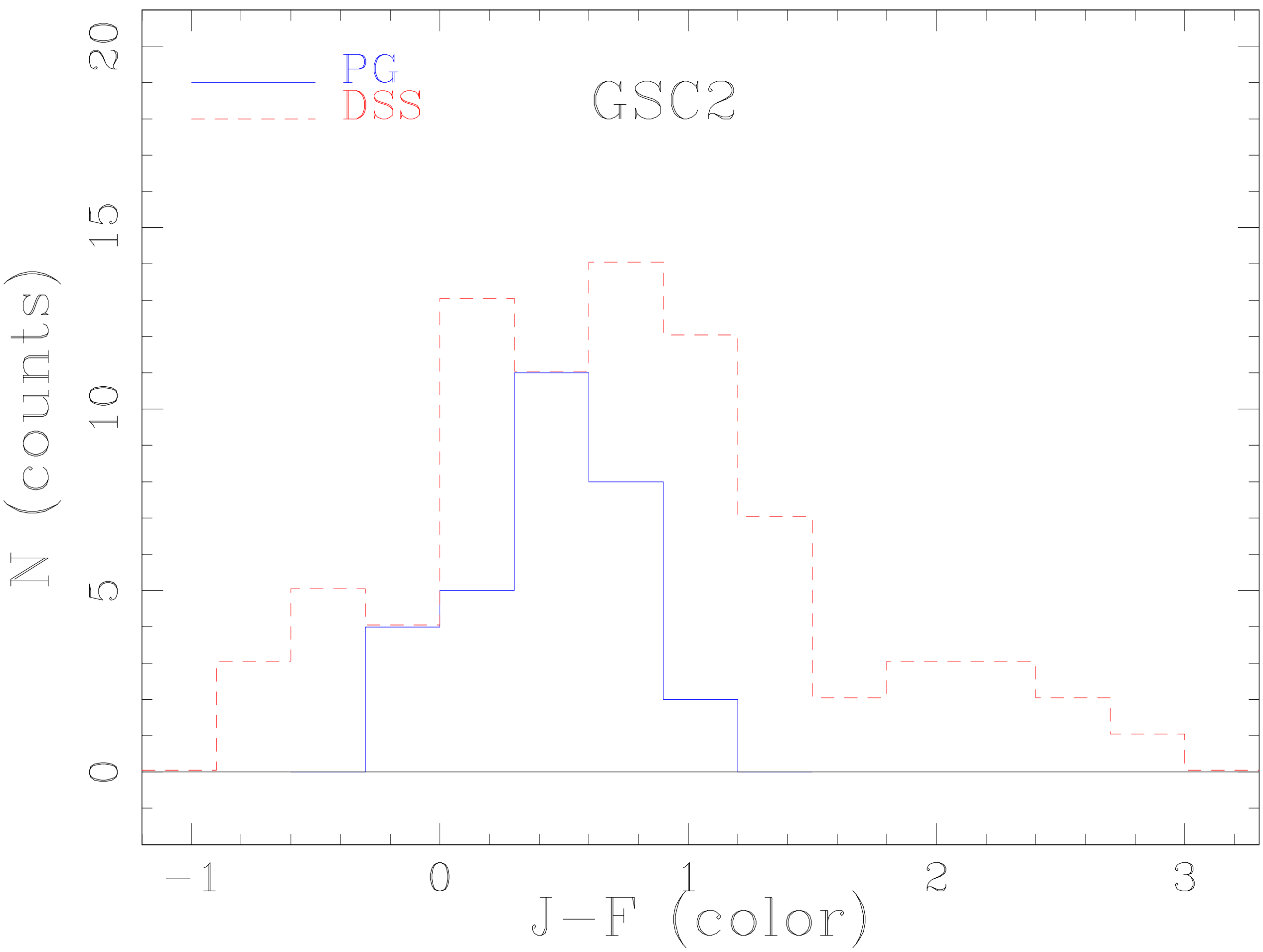

Fig. 13.— The $J - F$ color distribution for AGN in our Southern Sample and for QSOs belonging to the PG survey (Schmidt & Green 1983). A simple optical color selection $J - F \leq 1.0$, would decrease dramatically the completeness by a factor of 28%. Histograms are shifted slightly in y direction for clarity.

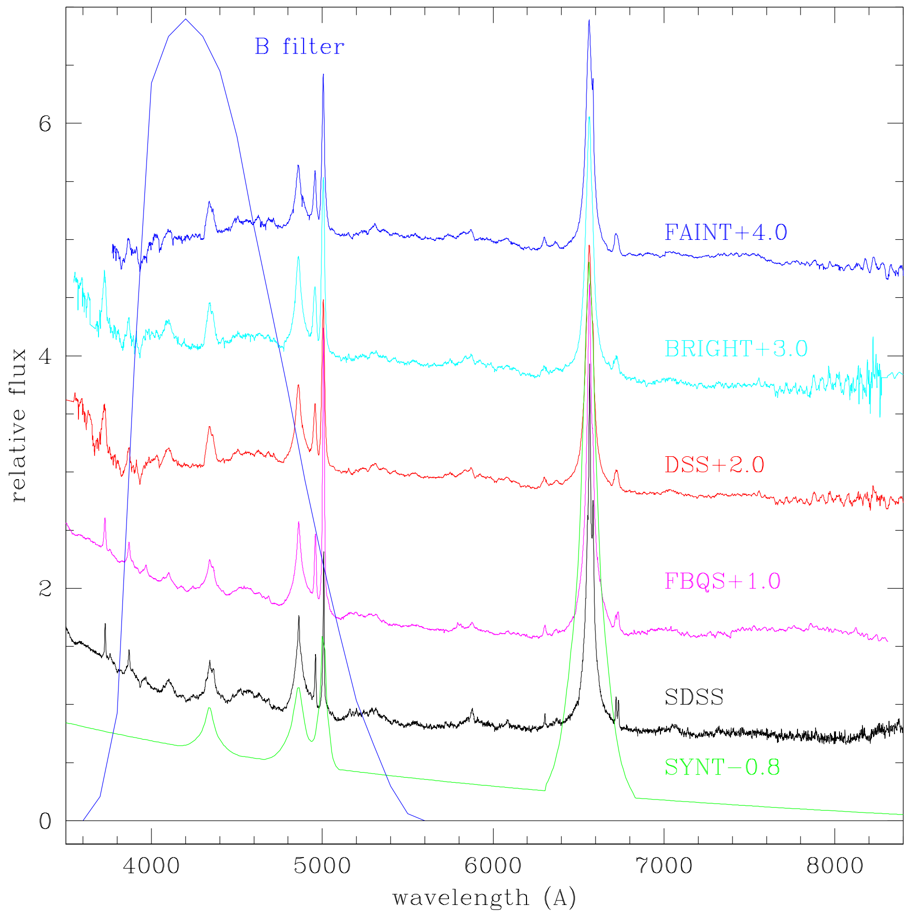

Fig. 14.— The composite QSO spectra of this survey (DSS), of the First Bright QSO Survey (FBQS), of the Sloan Survey (SDSS) and a synthetic spectrum (SYNT) with $f_\nu \propto \nu^{-1.75}$, typically used in photometric redshift studies. The composite spectra of bright ($M_B \leq -24$, BRIGHT) QSOs in this survey is clearly different from the composite spectra of faint ($M_B \geq -24$, FAINT) ones. The spectra are shifted by a constant value (+4.0 for FAINT, +3.0 for BRIGHT, +2.0 for DSS, +1.0 for FBQS and -0.8 for SYNT) for clarity.

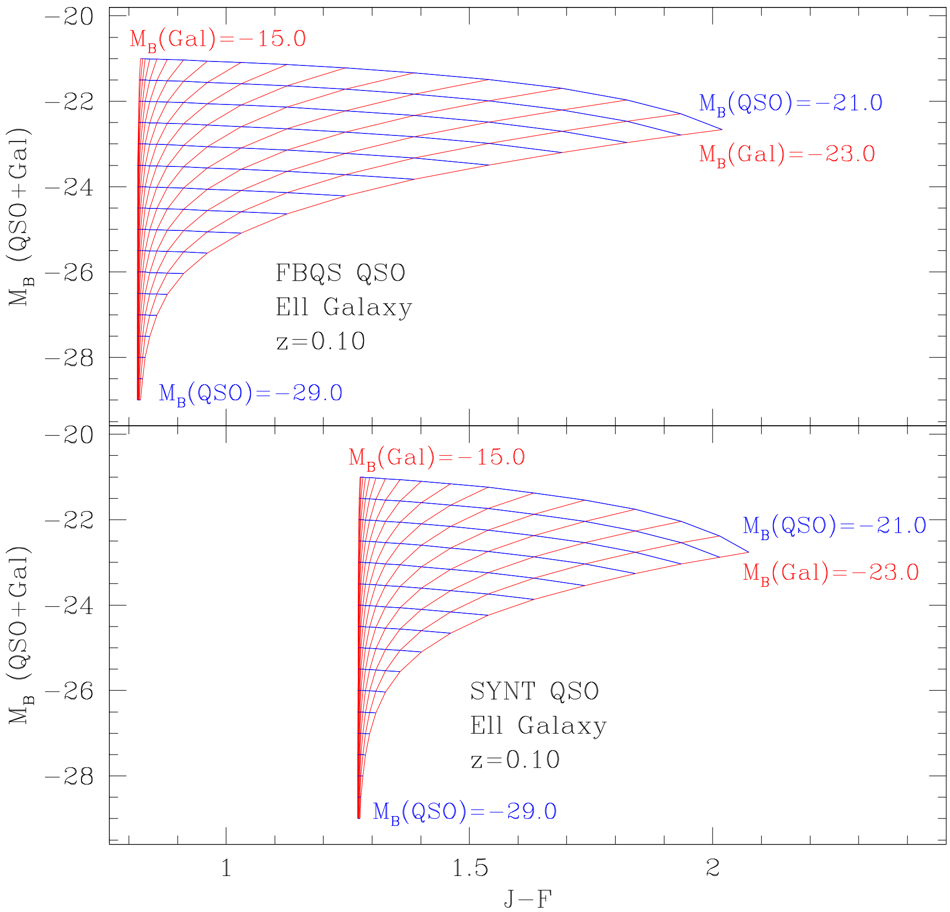

Fig. 15.— A synthetic $J - F$ vs. M_B diagram for FBQS (up) and for SYNT (down) QSO composite spectrum contaminated by an Elliptical galaxy, for different value of QSO and host galaxy Absolute Magnitude. Horizontal and vertical lines represent constant QSO and galaxy magnitudes, respectively.

Table 1. The AERQS Southern Sample.

Name (1RXS)	*R.A.*	Declination	B_J	z	Type
J000154.2-670749	00 01 55.05	-67 07 43.43	14.67	0.0000	STAR
J000307.6-180550	00 03 07.89	-18 05 50.17	13.28	0.0543	BLLAC
J001010.2-044225	00 10 10.77	-04 42 35.39	14.05	0.0295	AGN
J001020.5-061703	00 10 19.99	-06 17 06.40	15.01	0.0780	AGN
J001042.0-203916	00 10 42.65	-20 39 03.56	14.14	0.0000	STAR
J001410.1-071200	00 14 10.22	-07 11 56.76	13.84	0.0000	STAR
J001557.5-163659	00 15 58.51	-16 36 57.42	14.56	0.0000	STAR
J001936.2-071325	00 19 36.54	-07 13 24.10	13.93	0.0000	STAR
J002108.1-190950	00 21 07.53	-19 10 05.31	14.86	0.0952	GAL
J002246.1-380635	00 22 45.66	-38 06 53.14	15.04	0.1190	EM GAL
J002252.2-121233	00 22 51.51	-12 12 31.83	14.76	0.0000	STAR
J002339.6-175352	00 23 39.39	-17 53 53.16	14.85	0.0535	AGN
J002355.9-180254	00 23 55.37	-18 02 49.53	14.80	0.0530	AGN
J002750.4-323317	00 27 50.00	-32 33 06.12	14.13	0.0000	STAR
J003041.2-132130	00 30 40.18	-13 21 29.95	14.56	0.0760	AGN
J003322.1-691502	00 33 20.83	-69 15 14.06	14.21	0.0977	GAL
J003400.9-335428	00 34 01.66	-33 54 22.07	15.04	0.1180	AGN
J003908.2-222002	00 39 08.16	-22 20 02.14	14.00	0.0644	GAL
J004053.2-074201	00 40 52.75	-07 42 09.11	13.05	0.0560	AGN
J004131.9-223834	00 41 32.03	-22 38 38.36	13.24	0.0630	AGN
J004236.9-104919	00 42 36.84	-10 49 21.93	13.80	0.0413	AGN
J004423.9-261600	00 44 23.79	-26 16 06.35	14.60	0.0610	AGN
J004426.0-274848	00 44 25.39	-27 48 57.96	14.57	0.0000	STAR
J004554.8-172325	00 45 54.71	-17 23 28.72	14.69	0.0970	EM GAL
J005011.3-033743	00 50 10.62	-03 37 53.62	14.62	0.0000	STAR
J005118.0-144751	00 51 17.63	-14 47 51.61	14.65	0.0910	AGN
J005620.1-093626	00 56 20.05	-09 36 31.10	13.58	0.1010	BLLAC
J005655.1-751349	00 56 55.12	-75 13 52.54	15.04	0.0740	AGN
J005720.4-222300	00 57 20.16	-22 22 56.50	13.41	0.0620	AGN
J005822.8-024126	00 58 22.30	-02 41 42.43	14.43	0.0728	AGN
J010434.1-235919	01 04 33.90	-23 58 29.31	14.85	0.1596	GAL

Table 1—Continued

Name (1RXS)	*R.A.*	Declination	B_J	z	Type
J010538.7-141610	01 05 38.86	-14 16 14.27	13.84	0.0670	AGN
J010607.2-235907	01 06 07.75	-23 59 31.52	14.86	0.0000	STAR
J010818.9-413319	01 08 18.83	-41 33 08.03	13.33	0.0647	AGN
J010921.4-172057	01 09 21.69	-17 21 03.28	14.22	0.0520	EM GAL
J011029.4-151018	01 10 28.94	-15 10 08.25	14.82	0.0000	STAR
J011123.8-052539	01 11 23.55	-05 25 39.07	14.68	0.0000	STAR
J011151.3-404538	01 11 51.20	-40 45 44.25	14.18	0.0540	AGN
J011350.0-145041	01 13 50.04	-14 50 46.46	13.13	0.0527	AGN
J011457.6-422445	01 14 57.65	-42 24 49.50	14.72	0.1240	AGN
J011501.3-340008	01 15 01.47	-33 59 26.88	13.98	0.0000	STAR
J011724.1-222748	01 17 24.37	-22 27 59.97	14.70	0.1180	EM GAL
J011811.6-265819	01 18 10.63	-26 58 46.81	14.71	0.0000	STAR
J012020.1-102510	01 20 18.81	-10 25 30.40	14.90	0.0000	STAR
J012021.9-051052	01 20 21.97	-05 10 48.18	14.99	0.0470	GAL
J012059.4-270133	01 20 58.47	-27 01 44.29	13.90	0.0539	GAL
J012149.3-135810	01 21 49.95	-13 58 10.02	14.66	0.0550	AGN
J012151.5-282048	01 21 51.53	-28 20 57.34	14.39	0.1170	AGN
J012250.4-243937	01 22 50.49	-24 39 44.35	15.12	0.0000	STAR
J012448.3-115823	01 24 48.30	-11 58 08.87	14.93	0.0680	AGN
J012749.6-265036	01 27 50.17	-26 50 40.85	14.92	0.1090	AGN
J012806.9-184837	01 28 06.71	-18 48 31.10	13.14	0.0430	AGN
J013020.0-255710	01 30 20.41	-25 57 10.69	14.52	0.0000	STAR
J013445.2-043017	01 34 45.65	-04 30 13.61	14.87	0.0790	AGN
J013449.4-025441	01 34 50.33	-02 54 41.29	14.36	0.0000	STAR
J013514.2-071254	01 35 13.61	-07 12 49.72	14.19	0.0000	STAR
J013635.8-080617	01 36 35.53	-08 06 06.87	15.11	0.1461	GAL
J013655.2-064731	01 36 54.62	-06 47 34.04	15.03	0.0000	STAR
J014132.8-152755	01 41 32.53	-15 28 01.88	13.64	0.0820	AGN
J014345.1-060239	01 43 44.93	-06 02 39.34	14.04	0.0000	STAR
J014442.0-221339	01 44 40.43	-22 13 46.60	14.52	0.2780	GAL
J014841.1-483057	01 48 40.62	-48 30 51.48	13.78	0.0000	STAR

Table 1—Continued

Name (1RXS)	*R.A.*	Declination	B_J	z	Type
J015211.3-210737	01 52 11.34	-21 07 42.46	14.82	0.1040	EM GAL
J015227.1-231956	01 52 27.06	-23 19 53.90	14.50	0.1130	AGN
J015440.5-270659	01 54 40.26	-27 07 00.52	14.83	0.1510	AGN
J015503.5-050835	01 55 02.96	-05 08 34.55	15.10	0.1290	AGN
J015948.9-035206	01 59 49.04	-03 52 00.34	15.12	0.0000	STAR
J020013.6-084106	02 00 12.39	-08 40 48.90	13.46	0.0000	STAR
J020058.2-621451	02 01 01.48	-62 14 34.18	14.92	0.0000	STAR
J020515.9-450100	02 05 16.47	-45 01 02.79	14.90	0.1192	GAL
J020952.1-631838	02 09 50.73	-63 18 39.92	14.69	0.0000	STAR
J020953.8-135321	02 09 53.77	-13 53 20.87	13.88	0.0730	AGN
J021125.9-401702	02 11 24.82	-40 17 27.45	14.50	0.1050	GAL
J021220.1-444045	02 12 19.04	-44 41 05.54	15.03	0.0000	STAR
J021411.4-473241	02 14 11.86	-47 32 53.95	15.07	0.0000	STAR
J021438.0-643018	02 14 36.49	-64 30 17.50	13.79	0.0000	STAR
J021559.9-092913	02 15 58.64	-09 29 09.92	13.22	0.0000	STAR
J021738.8-300455	02 17 38.15	-30 04 48.29	14.99	0.0800	AGN
J022039.7-263441	02 20 41.84	-26 34 47.24	15.12	0.0000	STAR
J022225.7-411553	02 22 25.14	-41 15 52.27	14.83	0.0680	GAL
J022742.2-335351	02 27 42.34	-33 53 48.88	14.12	0.0000	STAR
J022901.8-153856	02 29 01.71	-15 38 54.10	14.88	0.0590	AGN
J023343.2-221744	02 33 45.11	-22 17 44.20	14.87	0.0000	STAR
J023400.1-181155	02 33 59.64	-18 11 51.90	14.83	0.0000	STAR
J023434.1-520359	02 34 34.31	-52 03 55.26	14.79	0.1370	AGN
J023849.4-403844	02 38 48.90	-40 38 39.05	13.18	0.0620	AGN
J024115.7-480733	02 41 17.34	-48 07 37.02	14.64	0.0000	STAR
J024146.8-525943	02 41 47.12	-52 59 30.19	12.86	0.0000	STAR
J024515.7-462754	02 45 13.36	-46 27 19.70	14.62	0.0920	GAL
J024554.2-445942	02 45 51.83	-44 59 44.95	15.09	0.0000	STAR
J024853.5-340428	02 48 52.45	-34 04 25.72	14.61	0.0000	STAR
J025126.1-245653	02 51 24.83	-24 56 39.51	14.18	0.1130	GAL
J025407.6-413731	02 54 07.04	-41 37 32.44	14.76	0.1460	AGN

Table 1—Continued

Name (1RXS)	*R.A.*	Declination	B_J	z	Type
J031521.0-564246	03 15 21.35	-56 42 51.19	14.91	0.0730	AGN
J031920.9-414639	03 19 20.22	-41 46 39.04	14.40	0.0810	AGN
J032214.3-664714	03 22 11.55	-66 47 28.86	15.01	0.0980	GAL
J032315.7-493113	03 23 15.28	-49 31 06.38	13.66	0.0710	AGN
J032521.8-563543	03 25 23.58	-56 35 45.45	13.97	0.0610	GAL
J033307.5-135419	03 33 07.77	-13 54 33.19	13.80	0.0390	AGN
J033424.5-151325	03 34 24.53	-15 13 40.69	13.45	0.0350	AGN
J033451.2-534242	03 34 51.53	-53 42 38.19	14.94	0.0613	GAL
J033648.2-554519	03 36 47.75	-55 45 12.61	15.03	0.0000	STAR
J033807.3-553558	03 38 06.27	-55 36 00.39	13.27	0.0590	AGN
J033823.5-451057	03 38 23.24	-45 10 49.22	14.97	0.1190	AGN
J034039.1-524301	03 40 38.35	-52 42 59.55	14.75	0.0000	STAR
J034117.1-225228	03 41 15.93	-22 52 43.14	14.13	0.0000	STAR
J034716.3-044419	03 47 16.34	-04 44 15.86	14.90	0.0000	STAR
J034930.8-534439	03 49 32.40	-53 44 09.09	14.72	0.0000	STAR
J035432.5-134005	03 54 32.81	-13 40 08.33	15.09	0.0766	AGN
J040126.6-080143	04 01 26.30	-08 01 59.92	14.59	0.1470	AGN ?
J040748.7-121133	04 07 48.42	-12 11 36.67	14.64	0.5740	AGN
J040805.1-273136	04 08 05.48	-27 31 38.31	14.55	0.0000	STAR
J040913.8-112455	04 09 13.51	-11 25 02.43	14.58	0.0920	AGN
J041417.0-090650	04 14 16.93	-09 06 48.82	14.45	0.0000	STAR
J041420.6-594134	04 14 19.05	-59 41 32.14	15.02	0.0710	AGN
J041530.5-661937	04 15 30.42	-66 19 19.85	14.66	0.0000	STAR
J041756.9-382649	04 17 57.33	-38 27 02.80	14.51	0.0000	STAR
J042202.2-415324	04 22 01.90	-41 53 28.86	14.13	0.0621	AGN
J042947.7-305240	04 29 43.69	-30 52 54.30	14.21	0.0000	STAR
J043153.6-585218	04 31 50.31	-58 52 12.17	14.86	0.0000	STAR
J043520.2-780150	04 35 16.29	-78 01 56.59	13.05	0.0610	AGN
J043726.6-471118	04 37 28.08	-47 11 29.43	13.97	0.0520	AGN
J044154.5-082639	04 41 54.00	-08 26 34.33	14.49	0.0440	AGN
J044404.7-222441	04 44 03.94	-22 24 46.30	14.94	0.0760	AGN

Table 1—Continued

Name (1RXS)	*R.A.*	Declination	B_J	z	Type
J044708.2-265731	04 47 07.78	-26 57 44.24	14.97	0.0000	STAR
J045230.4-295329	04 52 30.05	-29 53 35.20	15.04	0.2860	AGN
J045816.3-751608	04 58 17.19	-75 16 10.92	15.12	0.0000	STAR
J045851.2-190542	04 58 50.60	-19 06 04.32	14.52	0.0620	AGN
J045958.1-611506	04 59 57.74	-61 15 10.15	13.61	0.0860	AGN
J050054.7-511547	05 00 56.84	-51 16 30.68	13.97	0.1420	GAL
J050421.9-255420	05 04 22.05	-25 54 16.13	15.00	0.1200	AGN
J050903.4-420926	05 09 03.39	-42 09 21.92	14.64	0.0000	STAR
J051004.7-234024	05 10 04.17	-23 40 40.73	14.11	0.0000	STAR
J051949.5-454644	05 19 49.64	-45 46 44.15	13.70	0.0351	AGN
J052258.0-362729	05 22 57.96	-36 27 31.35	13.14	0.0553	AGN
J052815.9-294305	05 28 15.08	-29 43 03.04	14.95	0.1530	GAL
J052925.8-324858	05 29 25.38	-32 49 01.31	13.47	0.0000	STAR
J052945.2-323911	05 29 44.64	-32 39 14.58	15.11	0.0000	STAR
J053431.8-601613	05 34 31.03	-60 16 16.03	14.46	0.0570	AGN
J053509.9-390557	05 35 12.51	-39 06 05.65	14.83	0.0000	STAR
J053527.5-432247	05 35 26.78	-43 22 45.83	14.08	0.0650	AGN
J053555.0-653039	05 35 54.65	-65 30 38.67	14.80	0.0000	STAR
J053602.5-471844	05 36 02.87	-47 18 49.79	14.14	0.0000	STAR
J053621.3-514401	05 36 21.23	-51 44 08.20	14.69	0.1130	AGN
J053718.6-444257	05 37 18.66	-44 43 05.01	14.19	0.0990	AGN
J054105.5-615122	05 41 04.42	-61 51 50.68	14.99	0.0000	STAR
J055225.0-640206	05 52 24.54	-64 02 11.37	15.04	0.6800	AGN
J093444.7-060930	09 34 44.95	-06 09 19.44	13.97	0.0000	STAR
J095627.2-095720	09 56 26.41	-09 57 22.36	14.81	0.1610	GAL
J100802.7-145904	10 08 02.81	-14 59 05.93	13.57	0.0560	AGN
J100816.5-031526	10 08 16.60	-03 15 31.25	14.75	0.0000	STAR
J101438.9-084450	10 14 38.90	-08 45 20.27	14.99	0.0000	STAR
J101907.1-053703	10 19 07.26	-05 37 13.40	14.70	0.0747	AGN
J102225.1-142859	10 22 24.80	-14 28 57.61	15.05	0.0770	AGN
J102758.9-064804	10 27 58.68	-06 47 56.76	14.35	0.1165	AGN

Table 1—Continued

Name (1RXS)	*R.A.*	Declination	B_J	z	Type
J103727.1-111124	10 37 24.33	-11 11 56.00	14.42	0.0530	AGN
J103743.2-054848	10 37 43.85	-05 48 55.66	14.79	0.0000	STAR
J104115.4-210124	10 41 15.10	-21 01 25.21	13.26	0.0120	AGN
J104617.3-140206	10 46 17.08	-14 02 27.75	14.92	0.0680	AGN
J105421.2-092154	10 54 20.83	-09 21 56.52	13.62	0.0630	AGN
J112913.4-172114	11 29 14.18	-17 21 17.64	14.67	0.0000	STAR
J113104.6-094353	11 31 05.06	-09 43 53.72	14.55	0.0000	STAR
J113241.7-265155	11 32 41.50	-26 51 54.79	13.11	0.0000	STAR
J113301.6-153153	11 33 00.24	-15 31 51.56	14.60	0.0000	STAR
J113526.8-284040	11 35 26.14	-28 40 37.70	14.88	0.0820	AGN
J113546.6-093748	11 35 46.18	-09 37 58.37	14.91	0.1020	AGN
J113923.1-083241	11 39 21.93	-08 32 28.39	14.56	0.0000	STAR
J114042.0-174008	11 40 42.22	-17 40 10.38	12.94	0.0210	AGN
J114918.8-041649	11 49 18.64	-04 16 51.42	14.58	0.0850	AGN
J120246.0-034710	12 02 45.33	-03 47 21.48	14.49	0.0645	AGN
J120622.6-131453	12 06 21.90	-13 14 53.23	13.77	0.0000	STAR
J121027.7-131029	12 10 27.60	-13 10 08.51	14.87	0.0000	STAR
J131231.3-322847	13 12 30.72	-32 28 45.62	14.92	0.0000	STAR
J133910.9-212650	13 39 10.88	-21 26 52.15	14.39	0.0420	AGN
J134209.9-160020	13 42 11.40	-16 00 22.14	14.70	0.0000	STAR
J134951.0-131338	13 49 51.89	-13 13 38.03	15.05	0.0000	STAR
J135734.0-125433	13 57 33.20	-12 54 18.61	14.66	0.0581	GAL
J140329.8-084018	14 03 28.96	-08 40 23.84	14.92	0.0890	AGN
J141632.9-072529	14 16 33.15	-07 25 37.09	14.91	0.0000	STAR
J141817.0-211048	14 18 19.38	-21 11 12.01	14.13	0.1080	AGN
J142342.3-151550	14 23 42.03	-15 15 55.01	14.73	0.0000	STAR
J144111.3-021225	14 41 11.52	-02 12 35.28	14.94	0.0830	AGN
J144327.5-162029	14 43 30.09	-16 20 33.00	14.63	0.0000	STAR
J144427.6-042410	14 44 27.75	-04 24 03.60	14.77	0.0000	STAR
J150957.2-022554	15 09 57.82	-02 26 03.34	14.71	0.0000	STAR
J155542.1-102012	15 55 42.04	-10 20 00.09	14.68	0.0000	STAR

Table 1—Continued

Name (1RXS)	*R.A.*	Declination	B_J	z	Type
J201006.7-462206	20 10 06.86	-46 22 01.45	14.55	0.1050	AGN
J204644.0-114803	20 46 42.58	-11 48 10.84	14.84	0.0000	STAR
J205920.9-314733	20 59 20.72	-31 47 35.27	14.20	0.0740	AGN
J210134.8-410005	21 01 35.99	-40 59 51.94	14.35	0.0840	AGN
J210338.0-045548	21 03 37.89	-04 55 40.40	14.56	0.0620	AGN
J210736.5-130500	21 07 36.61	-13 04 54.44	13.75	0.0000	STAR
J210759.4-375400	21 07 59.77	-37 54 09.65	14.26	0.0490	AGN
J210910.1-094011	21 09 08.88	-09 40 18.55	12.65	0.0270	AGN
J211208.1-085004	21 12 11.17	-08 49 58.58	14.24	0.0000	STAR
J211244.3-373019	21 12 44.84	-37 30 12.24	13.77	0.0440	AGN
J211245.4-384025	21 12 45.09	-38 40 17.12	14.97	0.1430	AGN
J211551.4-104109	21 15 51.26	-10 41 22.27	14.51	0.0620	AGN
J212352.8-390819	21 23 52.79	-39 08 17.09	14.61	0.0000	STAR
J212401.9-002150	21 24 01.88	-00 21 58.46	14.77	0.0620	AGN
J212610.1-361813	21 26 07.60	-36 18 45.62	14.85	0.0000	STAR
J212951.7-022008	21 29 51.73	-02 20 06.04	14.52	0.0000	STAR
J213136.7-503704	21 31 36.15	-50 37 06.71	14.58	0.0750	AGN
J213135.7-120719	21 31 37.03	-12 07 24.64	14.11	0.5010	AGN
J213202.3-334255	21 32 02.25	-33 42 54.54	14.26	0.0300	AGN
J213623.1-622400	21 36 23.20	-62 24 00.47	13.54	0.0590	AGN
J213648.0-012407	21 36 49.40	-01 24 08.21	14.95	0.0000	STAR
J213704.1-340132	21 37 03.53	-34 01 05.41	15.06	0.0900	GAL
J214055.0-512516	21 40 54.17	-51 25 20.54	13.99	0.0970	AGN
J214334.0-250403	21 43 34.64	-25 04 07.47	15.03	0.1100	AGN
J214533.6-043434	21 45 33.39	-04 34 39.43	13.62	0.0690	GAL
J214701.2-214343	21 47 00.22	-21 43 24.49	14.72	0.0860	AGN
J215526.2-121025	21 55 27.79	-12 10 05.56	14.61	0.0000	STAR
J215830.1-094759	21 58 28.93	-09 47 49.81	14.08	0.0803	GAL
J220226.6-165755	22 02 26.47	-16 57 50.58	14.78	0.0000	STAR
J221142.4-204406	22 11 41.60	-20 44 15.11	14.81	0.0000	STAR
J221329.3-645512	22 13 29.53	-64 55 09.69	14.51	0.0710	AGN

Table 1—Continued

Name (1RXS)	*R.A.*	Declination	B_J	z	Type
J221504.1-033512	22 15 04.08	-03 35 26.66	14.82	0.0000	STAR
J221839.1-532639	22 18 40.42	-53 26 41.31	13.87	0.0000	STAR
J221959.6-505249	22 19 57.95	-50 53 04.13	14.98	0.0000	STAR
J223039.2-394246	22 29 47.72	-39 39 52.60	14.90	0.0730	GAL
J223046.8-423910	22 30 45.28	-42 38 52.01	14.98	0.0000	STAR
J223244.3-413441	22 32 43.16	-41 34 37.13	14.51	0.0750	AGN
J223455.4-605216	22 34 54.73	-60 52 10.60	14.28	0.0000	STAR
J224811.4-680322	22 48 09.31	-68 03 14.73	14.63	0.0960	AGN
J224841.4-510951	22 48 41.11	-51 09 53.43	14.69	0.1000	AGN
J225518.1-031040	22 55 17.93	-03 10 39.58	12.97	0.0000	STAR
J225923.7-503530	22 59 22.72	-50 35 31.75	14.17	0.0960	AGN
J230050.7-554549	23 00 52.03	-55 45 45.14	15.05	0.1420	AGN
J230152.0-550827	23 01 52.01	-55 08 30.91	14.84	0.1400	AGN
J230358.7-551717	23 03 57.97	-55 17 17.59	15.11	0.0840	AGN
J232046.5-672317	23 20 46.82	-67 23 18.97	14.65	0.0000	STAR
J232152.0-702645	23 21 51.16	-70 26 43.54	14.97	0.3000	AGN
J232857.5-680225	23 28 57.38	-68 02 32.49	13.94	0.0000	STAR
J233355.5-234336	23 33 55.23	-23 43 40.47	13.78	0.0480	AGN
J234032.5-263323	23 40 32.04	-26 33 19.37	12.89	0.0496	AGN
J234524.5-712645	23 45 21.95	-71 26 49.09	14.91	0.0000	STAR
J234842.8-735746	23 48 35.10	-73 57 33.99	14.36	0.0000	STAR
J234923.9-312602	23 49 23.94	-31 26 02.98	14.69	0.1350	AGN
J235555.3-132126	23 55 54.15	-13 21 24.80	14.67	0.0000	STAR
J235622.3-042949	23 56 19.77	-04 29 31.34	14.79	0.0000	STAR
J235720.0-125852	23 57 19.92	-12 58 49.98	14.27	0.0000	STAR
J235812.9-172437	23 58 12.97	-17 24 35.17	12.84	0.0000	STAR

Note. — R.A. is in $HH^hMM^mSS^s.SS$. Declination is in $DD^\circ PP^{'}SS^{``}.SS$. The coordinate system used is J2000. The classification and the redshift of J040126.6-080143 is uncertain, due to the low S/N of the spectrum.

Table 2. Area covered by AERQS. [The complete version of this table is in the electronic edition of the Journal. The printed edition contains only a sample.]

RA	DEC	l_{gal}	b_{gal}	$Expt$	Plate ID	Area
0.008333	-0.125000	96.477112	-60.35298	370.624	J794e	0.0625
0.008334	-0.375000	96.275253	-60.58234	373.924	J794e	0.0625
0.008334	-0.625000	96.070511	-60.81137	373.924	J794e	0.0625
0.008334	-0.875000	95.862831	-61.04010	368.425	J794e	0.0625
0.008335	-1.125000	95.652138	-61.26850	365.125	J794e	0.0625

Note. — RA is in decimal hours and DEC is in degrees. They are the central coordinates of small squares on the sky which satisfy the selection criteria described in § 3. l_{gal} and b_{gal} are the Galactic longitude and latitude. The coordinate system used is J2000. The exposure time (Expt) is in seconds. Plate ID comes from DSS and area is expressed in sq. deg.

Table 3. The Journal of the observations

Date	Telescope	Instrument	Slit	Resolution	Wavelength range
October 1998	2.3m Bok	B&C	$2''.5$	20 Å	5000-9000 Å
December 1999	2.3m Bok	B&C	$2''.5$	20 Å	5000-9000 Å
March 2001	3.5m TNG	DOLORES	$1''.5$	15 Å	4400-10000 Å
March 2001	1.54m Danish	DFOSC	$1''.5$	15 Å	3500-8500 Å
September 2001	1.54m Danish	DFOSC	$1''.5$	15 Å	3500-8500 Å

Note. — 2.3m Bok = Steward Observatory's 2.3m Bok Telescope at Kitt Peak National Observatory (KPNO); 3.5m TNG = Italian 3.5m National Telescope Galileo at Roque de Los Muchachos Observatory (ORM); 1.54m Danish = Danish-ESO 1.54m Telescope at La Silla Observatory. B&C = Boller & Chivens Spectrograph; DOLORES = Device Optimized for the LOw RESolution; DFOSC = Danish Faint Object Spectrograph and Camera.